

SIMULATION OF COMBUSTION AND THERMAL-FLOW INSIDE A PETROLEUM COKE ROTARY CALCINING KILN, PART 2: ANALYSIS OF EFFECTS OF TERTIARY AIRFLOW AND ROTATION

Zexuan Zhang
Research Assistant
Zzhang@uno.edu

Ting Wang
Professor
Twang@uno.edu

Energy Conversion and Conservation Center
University of New Orleans
New Orleans, LA 70148-2220, USA

ABSTRACT

A computational model is established to simulate the combustion and thermal-flow behavior inside a petcoke rotary calcining kiln. The results show that peak temperature is located at the tertiary air zone and a cold region that exists between the natural gas combustion zone and the tertiary air zone causes the coke bed to lose heat to the gas stream. The cold tertiary air injections reduce the gas temperature inside the kiln, so preheating the tertiary air using extracted gas or other waste energy is essential to saving energy. The devolatilization rate and location have a pronounced effect on the simulated temperature distribution.

As the calcining kiln rotates, the tertiary air injection nozzles will move relative to the coke bed and exert cyclic air-bed interactions. At zero angular position, the air injection nozzles are diametrically located away from the bed, so the interactions between the tertiary air jets and coke bed are minimal. As the kiln rotates to a 180-degree position, the stem of the air injection nozzles are actually buried inside the coke bed with the nozzles protruding outward from the bed. At this position, the tertiary air jets will provide a fresh layer of air just above the coke bed, and the interaction between the air flow and coke bed becomes strong. The 45° rotational angle case shows a better calcination with a 100 K higher bed surface temperature at the discharge end compared to the rest of rotational angles. Without including the coke fines combustion and the coke bed, the lumped gas temperature for the rotational cases shows a peak temperature of 1,400 K at $Z/D = 2$, which is due to natural gas combustion; the lowest temperature is around 1,075 K at two locations, $Z/D = 4$ and 8, respectively. The exhaust gas temperature is approximately 1,100K.

INTRODUCTION

Part 1 of this paper established the computational model for the study. Due to the complexity of the results, only the results of various rotational angles are presented in Part 2.

Other results will be presented in a future paper. For the convenience of reading Part 2, the locations and labeling of the tertiary air injectors are shown again here in Fig. 1.

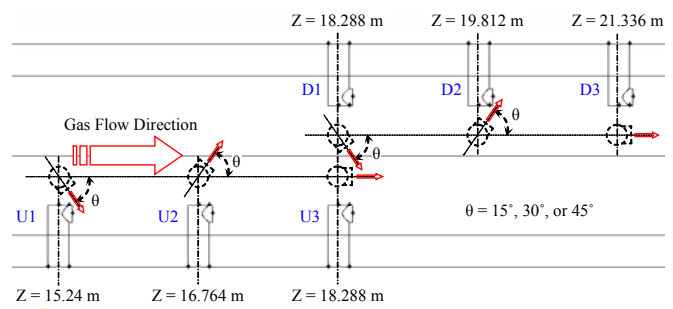


Fig. 1 Tertiary air injector locations and labeling (same as Fig. 13 in Part 1)

RESULTS AND DISCUSSIONS

Baseline Case (Case 1)

In the baseline case, the tertiary inlet is at the 0 degree position (see Fig. 9a in Part 1), and the tertiary air injection angles of D1, D2, U1 and U2 are ± 15 degrees (Fig.1). The entire kiln wall is set as the adiabatic wall condition. The combustion consists of all three types of reactions, natural gas with air, volatiles with air, and coke fines with air. The air is supplied with 23% oxygen and 76% nitrogen in mass fraction. In the heat-up zone, a thin layer is added above the coke bed acting as a heat sink that absorbs latent heat (347 kW/m^3) and simulates a moisture evaporation process. The simulation is carried out under a steady-state condition.

Figure 2a is a vertical plane view cutting through the middle of the kiln at $X = 0$. In this figure, the natural gas and the main air are supplied at the coke discharge end (left end of Fig. 2a). The combusted gas moves from left to right, and at the bottom the coke moves from right to left. The gas flow

direction (from left to right) is assigned as **the downstream** direction and opposite to the gas flow direction (from right to left) is assigned as **the upstream** direction. The natural gas combustion flame can be seen near the main air inlet with a flame temperature above 2,500 K. Downstream (toward the right) of this natural gas combustion region, a relatively cooler region with a temperature of around 1,000 K exists because of the depletion of natural gas and oxygen. In this relatively cooler zone, the coke bed surface temperature is calculated between 1,200 and 1,400 K (see Fig.2c), which is actually

higher than the gas temperature. This region is where the heat is lost from the coke bed to the gas. Moreover, this region is also where the quality of the calcined coke is critically dependent on the coke bed temperature. The current practice is to add natural gas combustion near the discharge end to maintain the required coke bed temperature and produce quality carbon products. However, as natural gas prices continue to be volatile and climbing, finding a means to reduce the natural gas consumption is an important operational goal to reducing production costs.

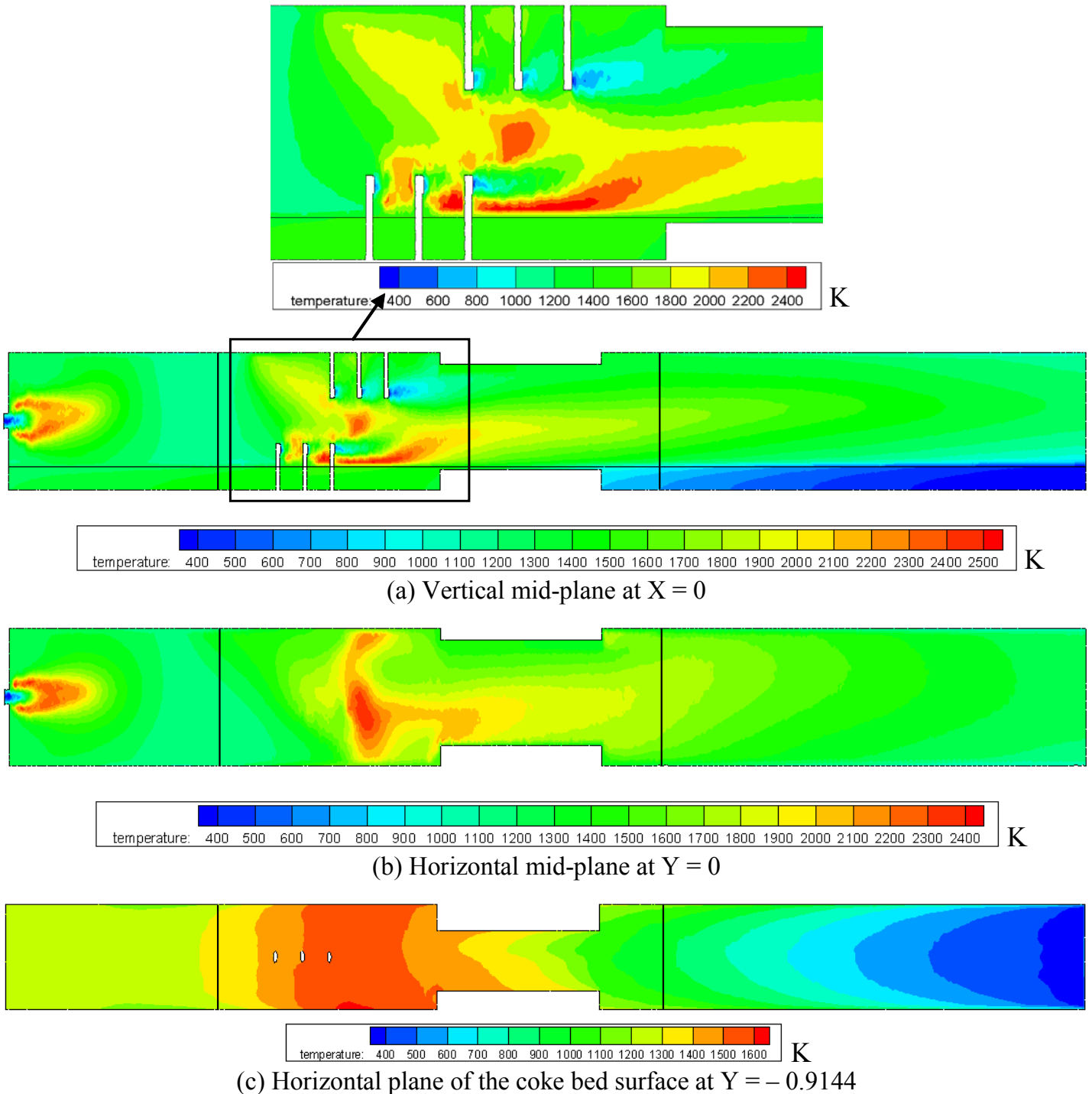


Fig. 2 Temperature contours inside the kiln for Case 1

In the tertiary air zone, volatiles that are devolatilized from the coke bed are combusting with the fresh injected air resulting in another high temperature region. At this region and in this figure, there are two groups of combustion flames present. The top flame is a result of the combustion of volatiles and coke fines (dusts) emitted from the coke bed with the air supplied from D1, D2, U1, and U2 tertiary air injectors. The bottom flame is created by the combustion of volatiles and coke fines with the air supplied solely by the U3 tertiary air injector. The cold air from the D3 tertiary air injector actually reduces the temperature in the tertiary air zone. This effect is clearly shown downstream of the D3 tertiary injector in Fig. 2a. In the heat-up zone, the heat sink embedded on the coke bed surface (between $Z = 36.576$ and 60.96 m) continuously absorbs latent heat from the main flow to vaporize moisture. This heat-sink effect can be observed by the reduced temperature at the layer right above the coke bed in Fig. 2a.

The temperature contours in Fig. 2a & b show an

interesting combustion pattern; the combustion takes place near the coke bed in the tertiary air injection region, but it lifts over to the center of the flow passage. Examination of the species concentration in Fig. 3 reveals this phenomenon is caused by a depletion of oxygen near the coke bed surface and a growing layer of unburned volatiles released from the coke bed. The oxygen concentration in Fig. 3a shows plenty of oxygen existing in the upper part of the kiln but is depleted in the lower part of the flow passage. The oxygen-rich air stream is somehow partitioned from the fuel (volatiles) rich gas by the combusted gas. Mass weighted mass fraction distributions in Fig. 4 also show about 14% (or 1% of the total gas mass) of the volatiles are not burned at gas exit (feed end) of the kiln. This simulated result provides an important insight into the combustion phenomenon, and hence, by increasing downstream mixing provides an opportunity for implementing a means to manipulate the flow to achieve a more effective combustion near the coke bed. This will be a worthwhile task for future study.

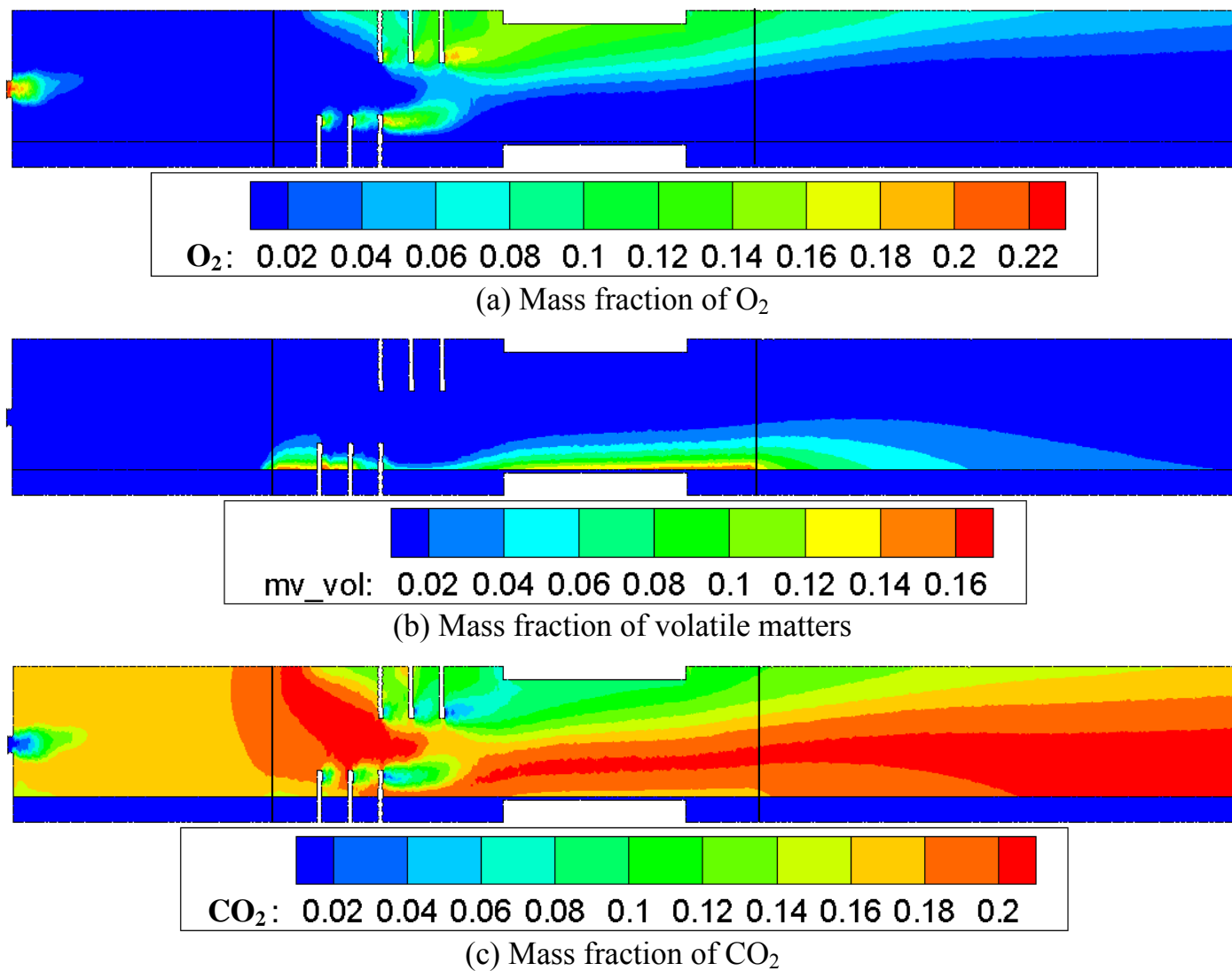


Fig. 3 Species mass fraction inside the kiln for vertical mid-plane at $x = 0$ for Case 1

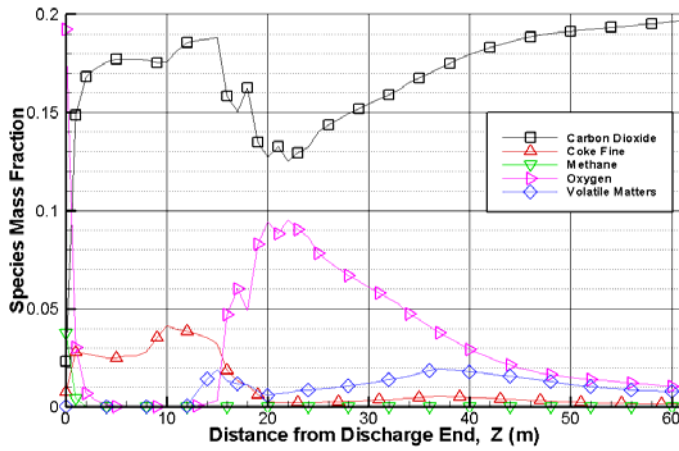


Fig. 4 Mass weighted species mass fraction distributions inside the kiln for Case 1

Some effects of the tertiary injection angle and arrangement can be observed in the horizontal mid-plane view of $Y = 0$ (Fig. 3b). In the calcining zone, the U1 tertiary air injector creates a combustion flame that goes up and the U2 tertiary air injector creates a relatively hot zone that moves

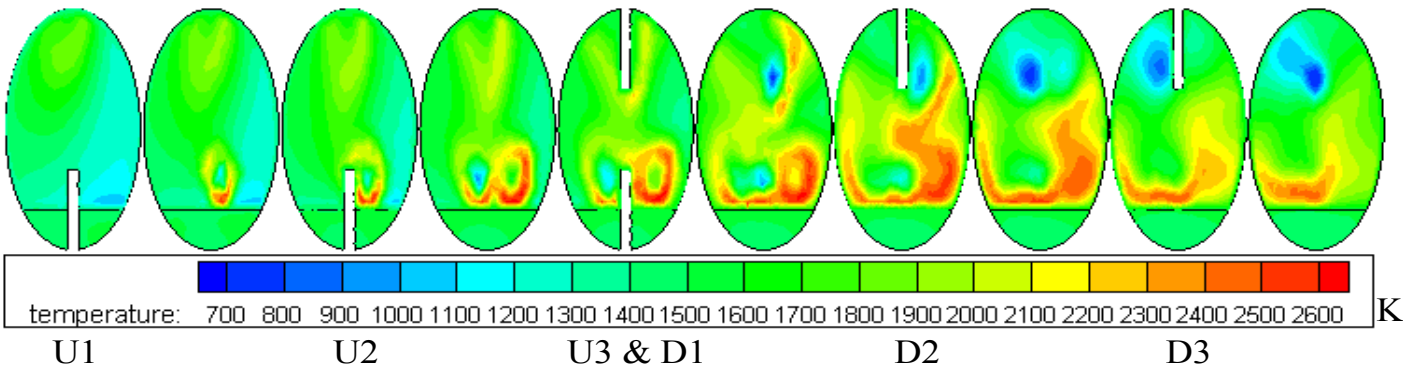


Fig. 5 Temperature contours at each tertiary air inlet location for Case 1

The temperature distribution along the centerlines ($X = 0$) of the gas region as well as three different depths in the coke bed (coke bed surface, in the mid-depth, and at the bottom) are shown respectively in Fig. 6. The centerline gas temperature shows that the peak temperature of the main inlet combustion is about 2,200 K at less than 5 m from the discharge end, and in the tertiary air inlet zone, the combustion peak temperature rises up to 2,300 K at $Z = 20$ m. Between these two peaks, the temperature drops below 1,150 K at the end of natural gas combustion zone at $Z = 10$ m. In this region of relatively cool gas temperature ($Z = 7 \sim 15$ m), the coke bed temperature is actually higher than the gas temperature, so heat is lost from the coke bed to the gas. Heat lost from the coke bed can be further supported by comparing the centerline temperature at three different depths: the temperature at the coke bed bottom is higher than in the mid-depth, which in turn has the temperature higher than on the coke bed surface, and the mass weighted average static temperature reaches around 1,800 K for natural gas combustion and volatiles combustion.

down. Figure 1c is the plane view for $Y = -0.9144$, which is the coke bed surface plane. Figure 2c shows the coke bed surface temperature gradually increases from the feed end (300 K) to as high as 1,600 K at the calcining zone and finalizes at 1,200 K at the discharge end.

Fig. 5 shows temperature contours of ten cross-sections cutting through the six tertiary inlet piping and downstream of the injectors. The cold air injected from the U1 tertiary air inlet reduces the temperature in its cross-sectional view. In the U2 cross-sectional view, the air from the U1 tertiary air inlet combusts with volatiles and coke fines right above the coke bed. The core of that air stream is still cold. In U3 cross-sectional view, the combustion is stronger, but it seems the combustion takes place on the shear layer surrounding the cold core of air stream. Stronger combustion is taking place in the D2 cross-sectional view, and again, cold air streams from the U3 and D1 tertiary air injections create relatively cold regions. The signature of the cold air stream core persists throughout the tertiary air injection region as can be seen in Fig. 2a and Fig. 5.

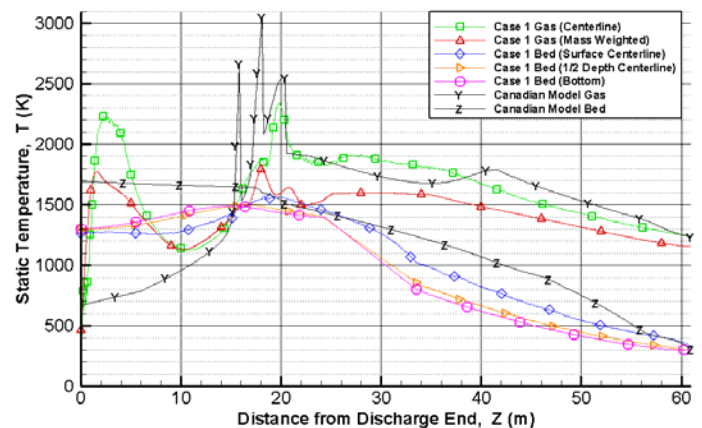


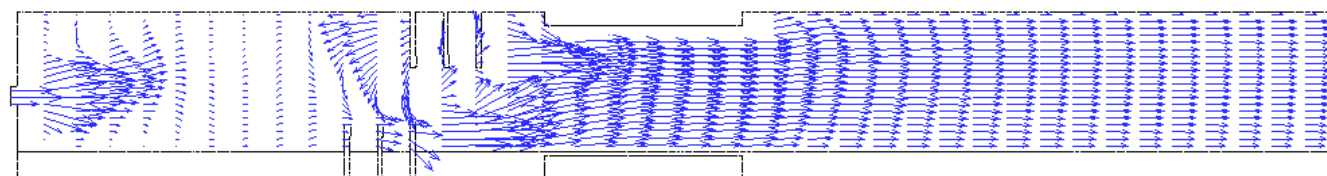
Fig. 6 Central line static temperatures for gas and coke bed for Case 1 including mass flow weighted gas temperature

The coke bed surface temperature starts cold at the feeding end ($Z = 60.96$ m) and reaches the maximum value of 1,500 K at around $Z = 15$ m; at the discharge end, the coke bed temperature becomes uniform and is discharged at about 1,300

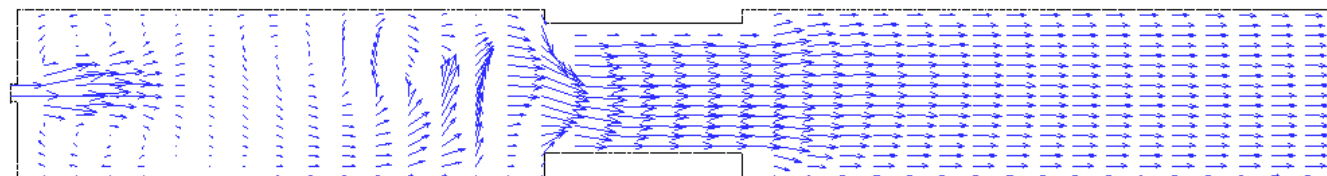
K. Starting from the feeding end, the coke bed surface always receives the heat from the hot gas and maintains at the hottest in the coke bed until the coke moves to the relatively cool gas region at $Z = 15$ m. Reversal of temperature gradient from receiving heat to losing heat is clearly shown at $Z = 16$ m in Fig. 6, where the coke bed surface temperature drops becoming the coolest in the coke bed.

Representative flow fields are shown in Fig. 7. From the flow field shown in the vertical mid-plane ($X = 0$) in Fig. 7a, a stagnant flow induced by recirculation can be seen between the discharge end and the tertiary air injection region.

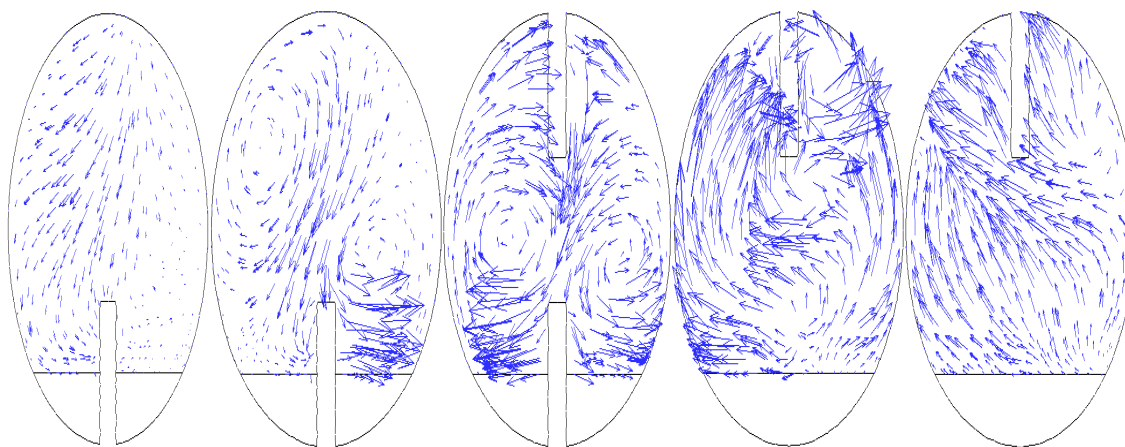
This recirculation flow is caused by the entrainment induced by the strong main flow entering momentum. This entrainment is so strong that even the air flow injected from the D1 tertiary injector is reversed (see Fig. 7c) and moves toward the discharge end. The combustion produced by the reversed tertiary flow can be seen in Fig. 2a upstream of the D1 tertiary air injector. The reversed flow is stopped by the main flow entering from the discharge end and forms a high-pressure stagnant region between $Z = 5$ and 15 m. It is here no combustion occurs, and the gas temperature reduces to below 1,150 K, as discussed earlier in Fig. 6, due to entrained cold tertiary air.



(a) Vertical mid-plane at $X = 0$



(b) Horizontal mid-plane at $Y = 0$



(c) Five tertiary air injection cross-sections

Fig. 7 Velocity profiles for Case 1

Various Rotational Angles

Case 1 was conducted with the tertiary air injection plane perpendicular to the coke bed surface as shown in Fig. 9a in Part 1. Note: Due to rotation the coke bed generally tilts approximately 15 degrees counterclockwise. For convenience and easy reading, Fig. 9 (Part 1) is plotted with a horizontal coke bed surface. Since the kiln is rotating, the relative positions of the tertiary air injectors with respect to the coke bed surface continuously changes. The result of thermal-flow fields and combustion pattern, due to the change of the tertiary air injection positions, are compared at five different positions: 0 (Case 5), 45 (Case 6), 90 (Case 9), 135 (Case 10), and 180 (Case 11) degrees, respectively. In this group of simulation, a specific interest is focused on whether the tertiary air injection

would disturb the coke bed, kick off coke particles, and result in increased attrition and reduced production. Since the detailed thermo-flow and combustion fields have been analyzed and discussed in Case 1, to shorten the computational time, the conjugate conduction calculation through the coke bed and combustion of coke on the coke bed are not included in other cases. Figure 8a, the vertical plane view of $X = 0$ for Case 5, shows a temperature field similar to the baseline case (Case 1), except the temperature is lower without including coke fines combustion. Cool air streams can be seen downstream of each injector. In Fig. 8b (45°) and Fig. 8c (90°), the temperature range is similar to Case 5, and these two positions produce similar temperature distributions. Since there is no tertiary injection on this plane, no cool air streams are observed.

Regions of hot combustion are seen across the entire kiln in the tertiary air injection area. Due to the release of volatile matters from the coke bed, the major combustion region is still located downstream of the tertiary air injections and near the lower part of the kiln. No obvious improvement of combustion is seen on the upper part of the kiln when the tertiary air is injected off from the vertical plane. The cool region between the natural gas combustion flame and the tertiary air injection region is about 100 K hotter than Case 5. The effectiveness of combustion for the tertiary air injection at

position 135° in Fig. 8d is significantly reduced from a similar position at 45° (Fig. 8b). Due to the switching of downstream and upstream locations of the upper and lower injectors, this combustion reduction seems to be solely caused by the effect of the flow field. The combustion is suppressed when the lower injectors are located downstream of the upper injectors. This observation is confirmed by the results of Case 11 shown in Fig. 8e, which occurs when the injectors are rotated 180° off from the baseline location shown in Fig. 8a.

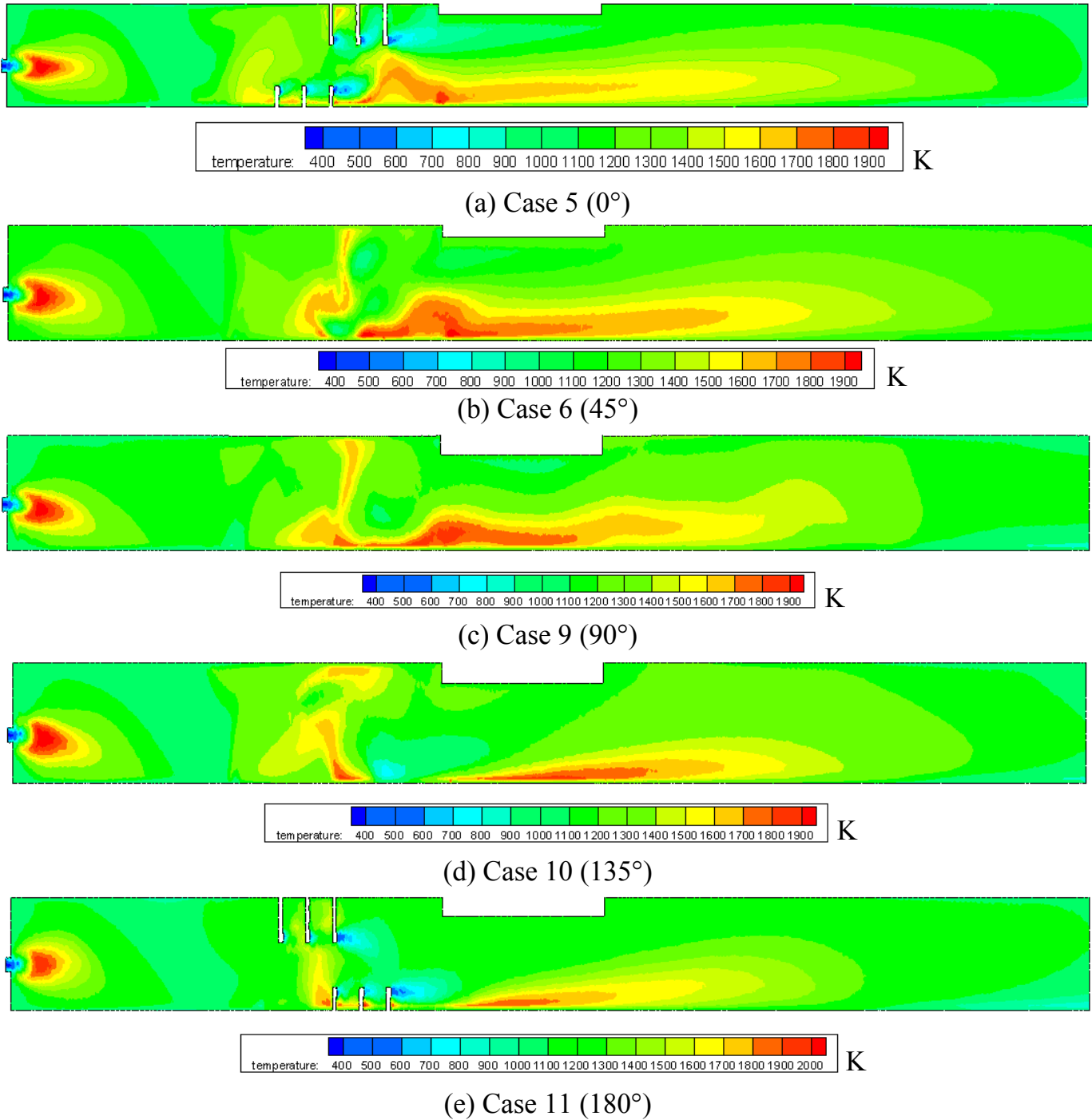


Fig. 8 Temperature contours on the vertical plane $x = 0$ for various rotational angles

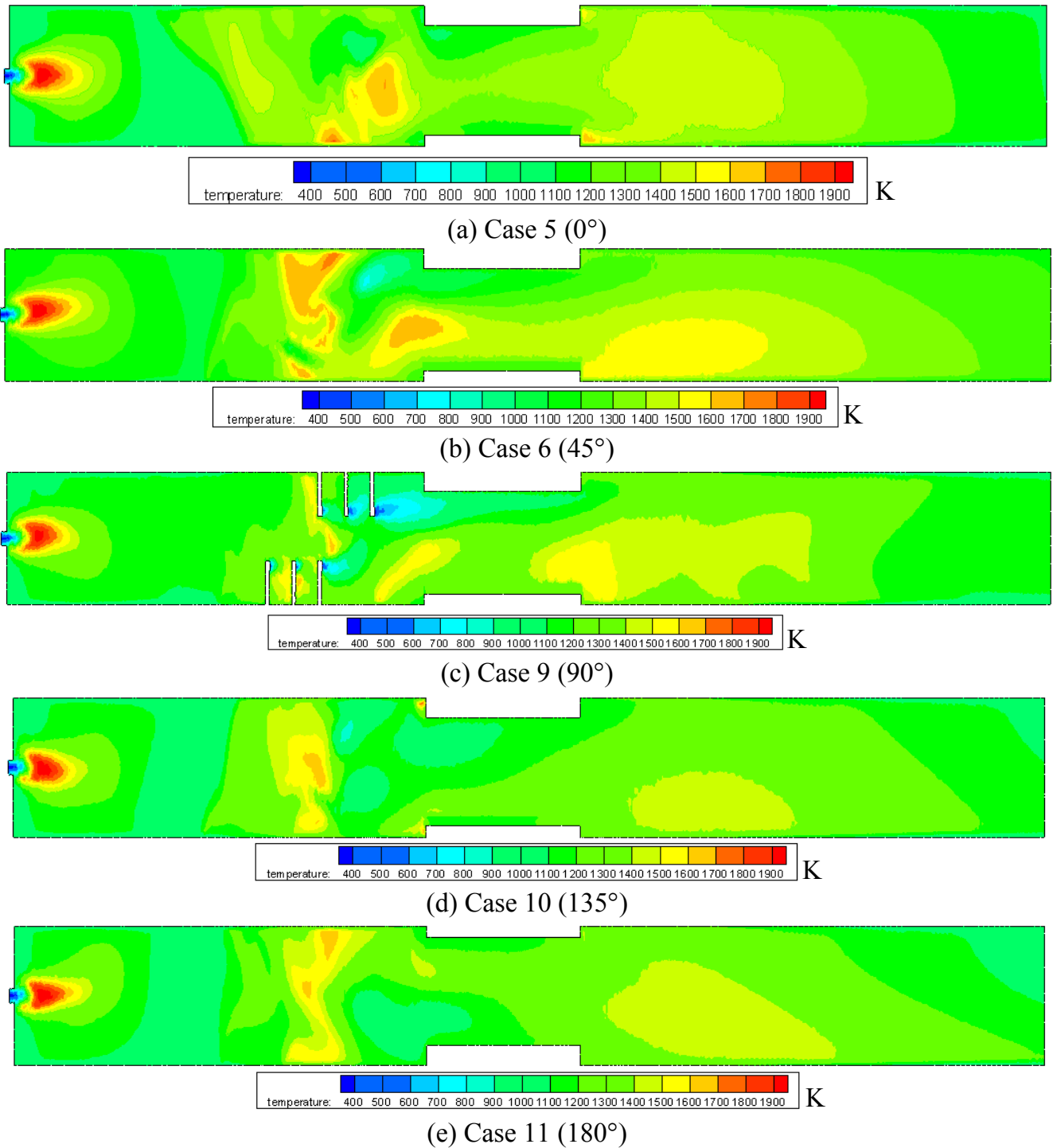


Fig. 9 Temperature contours on the horizontal mid-plane $y = 0$ for various rotational angles

Figure 9 shows the temperature contours on the horizontal mid-plane ($Y = 0$). The relatively lower temperature distribution when compared with the vertical temperature distribution in Fig. 8 indicates that the combustion is weaker on the mid-plane of the kiln. Case 6 (45°), in Fig. 9b, shows more combustion than other cases; while Case 9 (90°), in Fig. 9c, shows the lowest combustion activity on the mid-plane. Combination of the temperature contours on the vertical mid-plane in Fig. 8, and the horizontal mid-plane in Fig. 9 clearly indicates most of the combustion taking place near the lower part of the kiln near the coke bed.

As stated earlier, the off-center turning angles ($\pm 15^\circ$) of injectors D1, D2, U1, and U2 are made to direct the air streams away from hitting the downstream injectors. During rotation, two of these injectors will periodically blow air towards the coke bed. This will kick the coke dusts off from the coke bed surface and result in coke attrition and loss of product yields. In addition, tertiary air injections exert impacts on the coke bed surface temperature distribution. Although tertiary air provides oxygen to combust the volatiles, it also provides the cooling effect if it is directly blowing towards the bed surface. For example, the snapshot temperature contour in Case 10 (135°) in Fig. 10e shows a cool area between the third injector

(U3) and the tumbler, which is the evidence of the cooling effect of the off-center air jet blowing from D1. Again, the coke bed surface temperature between natural gas flame and tertiary inlet zone for Case 6 in Fig. 10b is 100 K higher than other four cases. Recall that the calculation of Cases 5-11 are conducted without including the coke bed, so temperature

distribution on the coke bed surface appears to be stripes rather than the bell shape as shown in Fig. 2c. Comparison among Figs. 2a, b, c with Figs. 8a, 9a, and 10a shows the effect of conjugate coke bed heat transfer on the coke bed temperature.

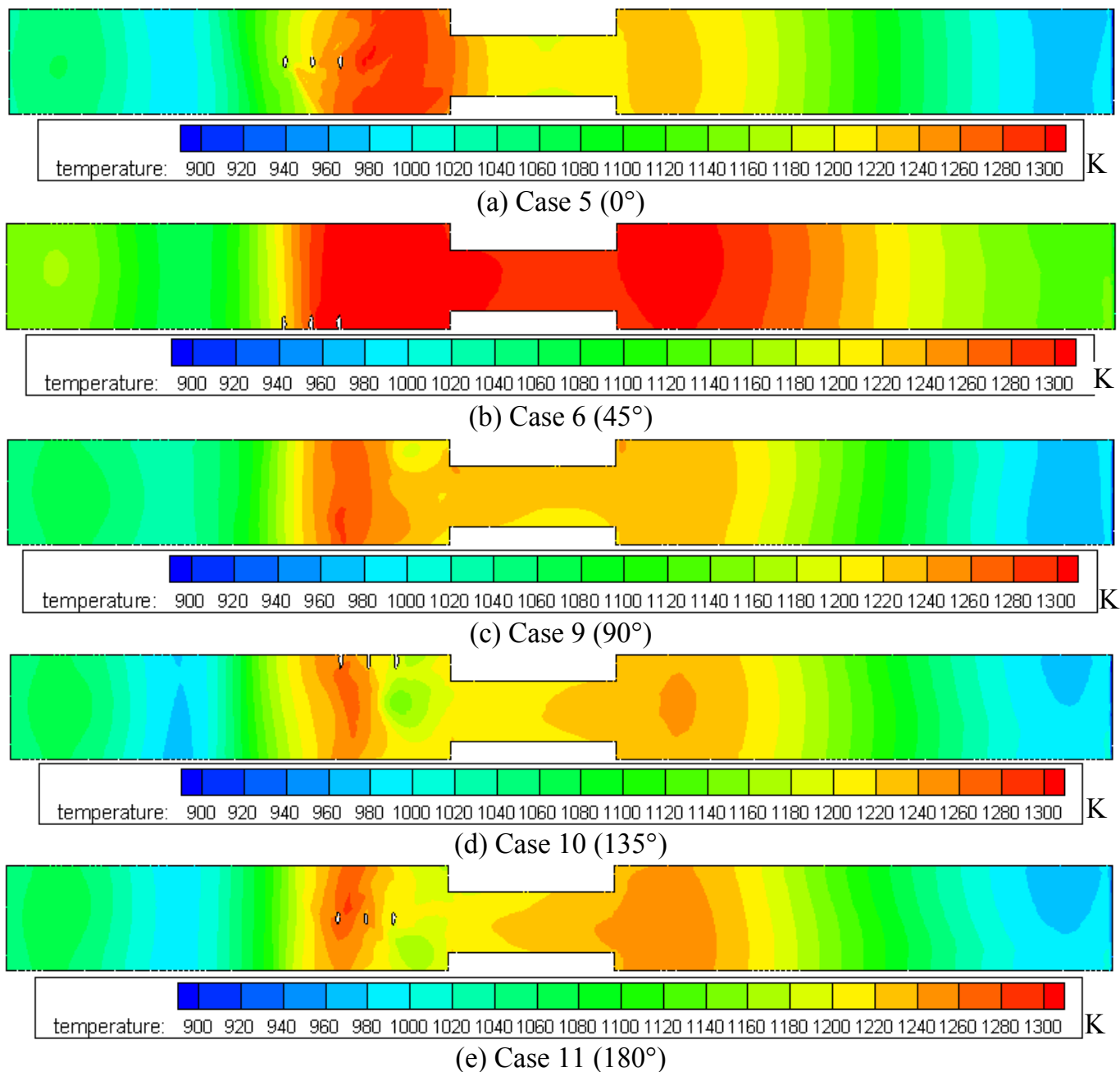


Fig. 10 Temperature contours of horizontal plane $y = -0.9144$ for various rotational angles

Figure 11 shows the temperature distribution at each tertiary air injection cross-section. The evolution of the temperature distribution at each tertiary injection location can be observed by looking at the same location with the rotational sequence. The cold air streams are evident in these sequential cross-sectional temperature contours. In Cases 10 (135°) and Case 11 (180°), the effect of cold stream prevails downstream of the injectors and results in the reduced combustion shown in Fig. 8 d and e. Since Figs. 8 and 9 only show selected planes

for comparison, what position produces the best or worst combustion performance is not clear. Mass flow weighted calculations of temperature by integrating over the cross-section at selected axial location are shown in Fig. 12a for five rotational cases. As expected, the temperature distribution near the discharge end shows negligible difference for all other rotational positions except at 45° rotational angle. The hot regions of tertiary air combustion vary depending on the tertiary air injection position.

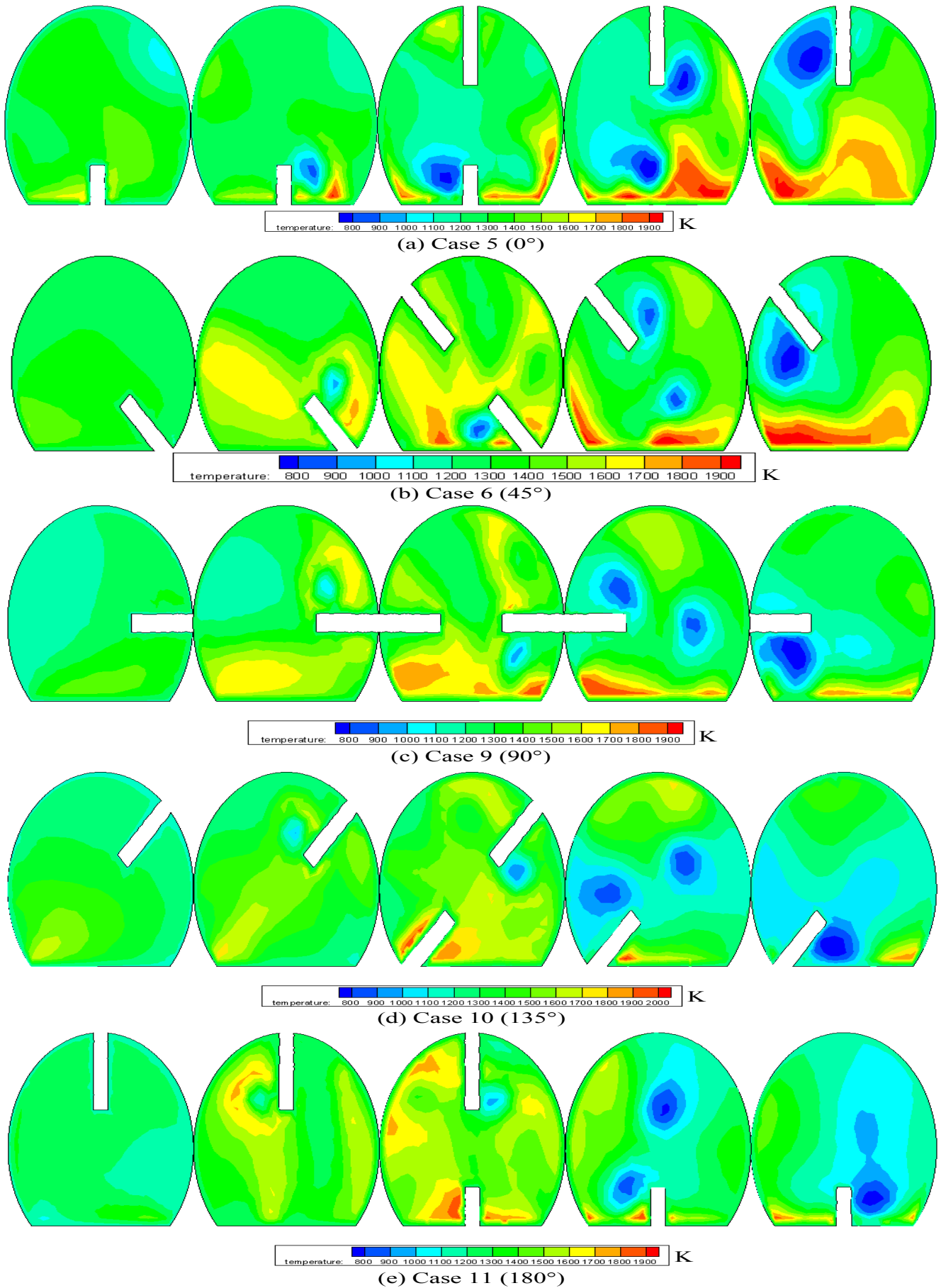


Fig. 11 Temperature contours at each tertiary air injection location for various rotational angles

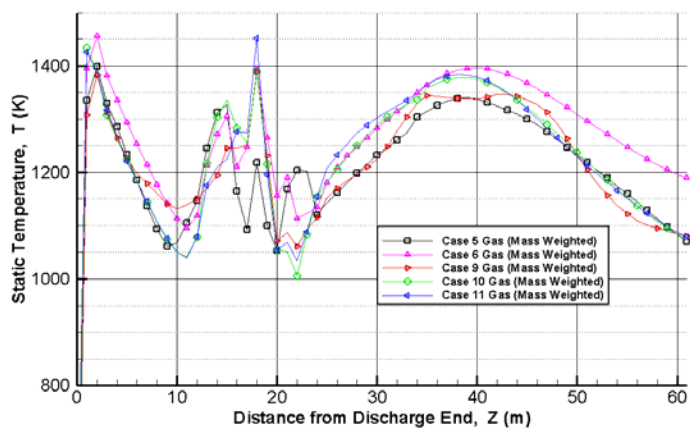
In a real situation, all the cases will occur in one rotation; the average value of these five cases (lumped value) in Fig. 12b gives a better description of the averaged temperature distribution along the kiln. Due to natural gas combustion, the peak temperature of the lumped gas is 1,400 K at around $Z = 2$ m location. At the tertiary air injection zone, peak combustion temperature occurs at $Z = 18$ m with highest temperature at about 1,370 K. Bed surface temperature of Case 6 (45°) is approximately 200 K higher than the other four positions as shown in Figs. 10 and 13. Because better combustion and the higher gas temperature of Case 6 (45°) has successfully heat up the coke bed, Case 6 is the best among the five studied rotating locations.

Mass flow weighted calculations of temperature and species mass fractions by integrating over the cross-section at the gas exit plane are shown in Table 1. Generally speaking, the cases showing higher temperature, higher CO_2 , lower O_2 , and lower volatiles are cases of better combustion. However, the data shown in Table 1 do not provide a clear picture on which case is the best because the data show Case 9 (90°) has the highest CO_2 production and least residual of O_2 , while Case 6 (45°) reaches the highest temperature, and Case 5 (0°) has the minimum unburned volatiles. Irrespective of the indecisiveness in determining which case is the best, it is relatively certain that Cases 10 and 11 (135° and 180°) do not perform as well as other cases. In a real situation, all the cases would occur in one rotation. The average values of these five cases in Table 1 would give a better description of the averaged overall performance of each rotation. It needs to be noted that the simulation does not model the phenomena of flow disturbance on the coke bed surface when the tertiary jets impinge on the coke bed surface and kick off the coke particles into the gas stream.

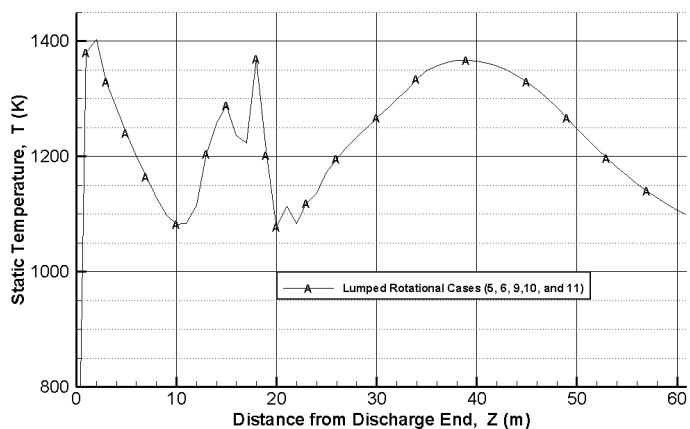
Table 1 Mass flow weighted average values at the feed end (or gas exist) for each rotational angle

Rotational Angle	Temperature (K)	CO_2 Mass Fraction	O_2 Mass Fraction	Volatiles Mass Fraction
0° (Case 5)	1070.44	0.1351	0.0495	3.00×10^{-05}
45° (Case 6)	1189.49	0.1427	0.0398	47.08×10^{-05}
90° (Case 9)	1080.11	0.1494	0.0311	3.84×10^{-05}
135° (Case 10)	1073.81	0.1413	0.0418	17.49×10^{-05}
180° (Case 11)	1078.75	0.1433	0.0393	33.84×10^{-05}
Total Average	1098.52	0.1423	0.0403	21.05×10^{-05}

Figures 14 and 15 show the streamwise (Z -direction) velocity profiles on the vertical and horizontal mid-planes, respectively. At the tumbler region, the higher velocity flow shifts from top to bottom from Case 5 to Case 11, following the position change of the tertiary air injections. Similar to Fig. 7, recirculation exists between the main inlet combustion flame and the tertiary air zone. The stagnant zones inhibit hot natural gas flame from moving further downstream. The cross section views of velocity profiles at each tertiary air injection location for all 5 rotational angles are shown in Fig. 16.



(a) Mass flow weighted average temperature for each rotational angle



(b) Lumped gas temperature for rotational cases

Fig. 12 Mass flow weighted average and lumped gas static temperature for various rotational angles

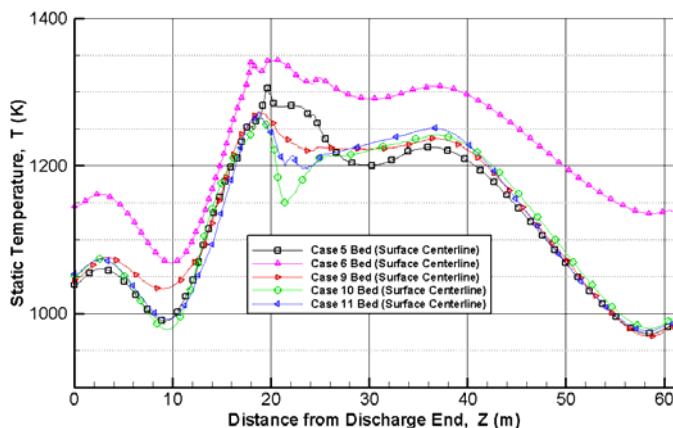


Fig. 13 Bed surface centerline static temperature for various rotational angles

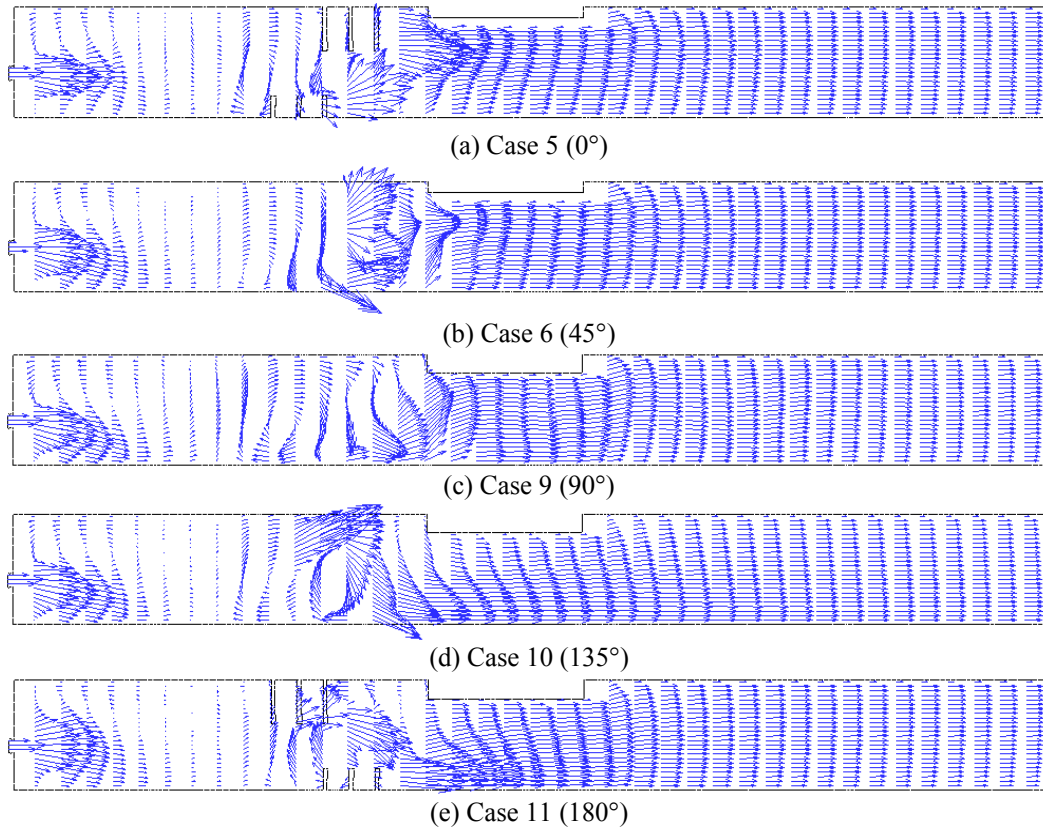


Fig. 14 Streamwise velocity profiles on the vertical plane $x = 0$ for various rotational angles

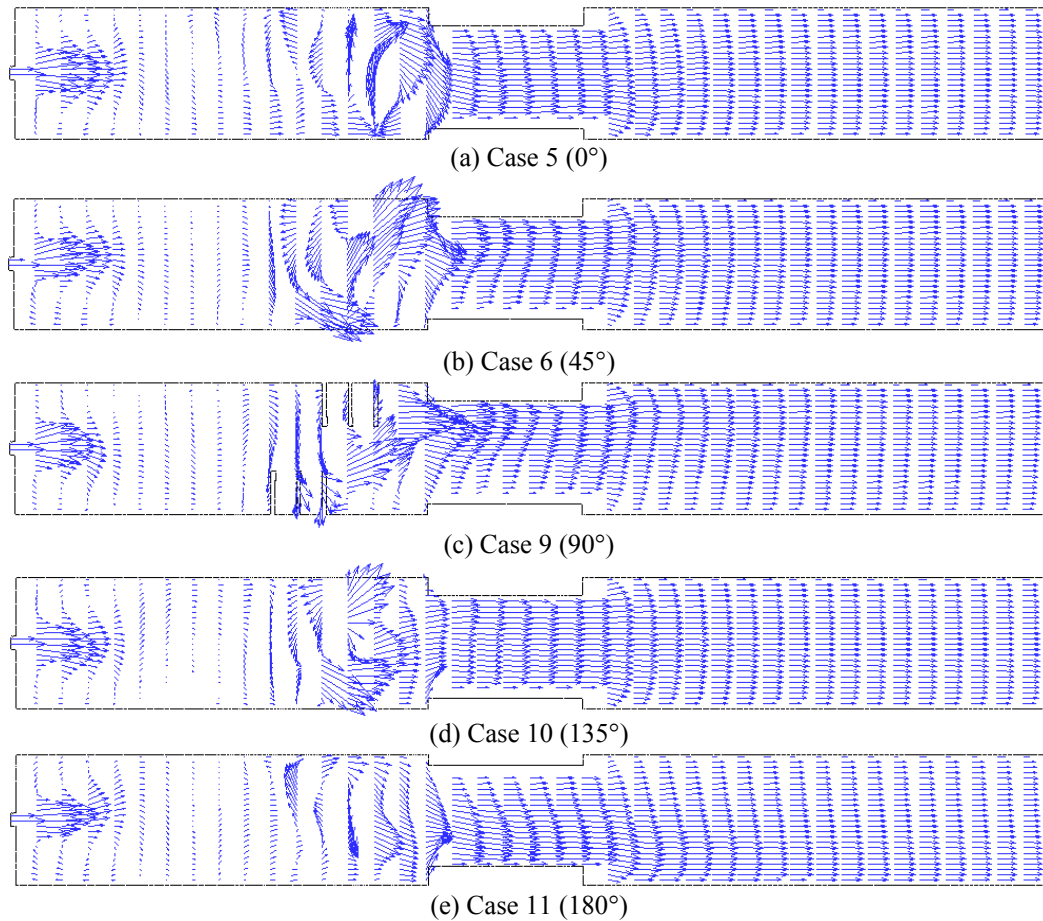


Fig. 15 Streamwise velocity profiles on the horizontal plane $y = 0$ for various rotational angles

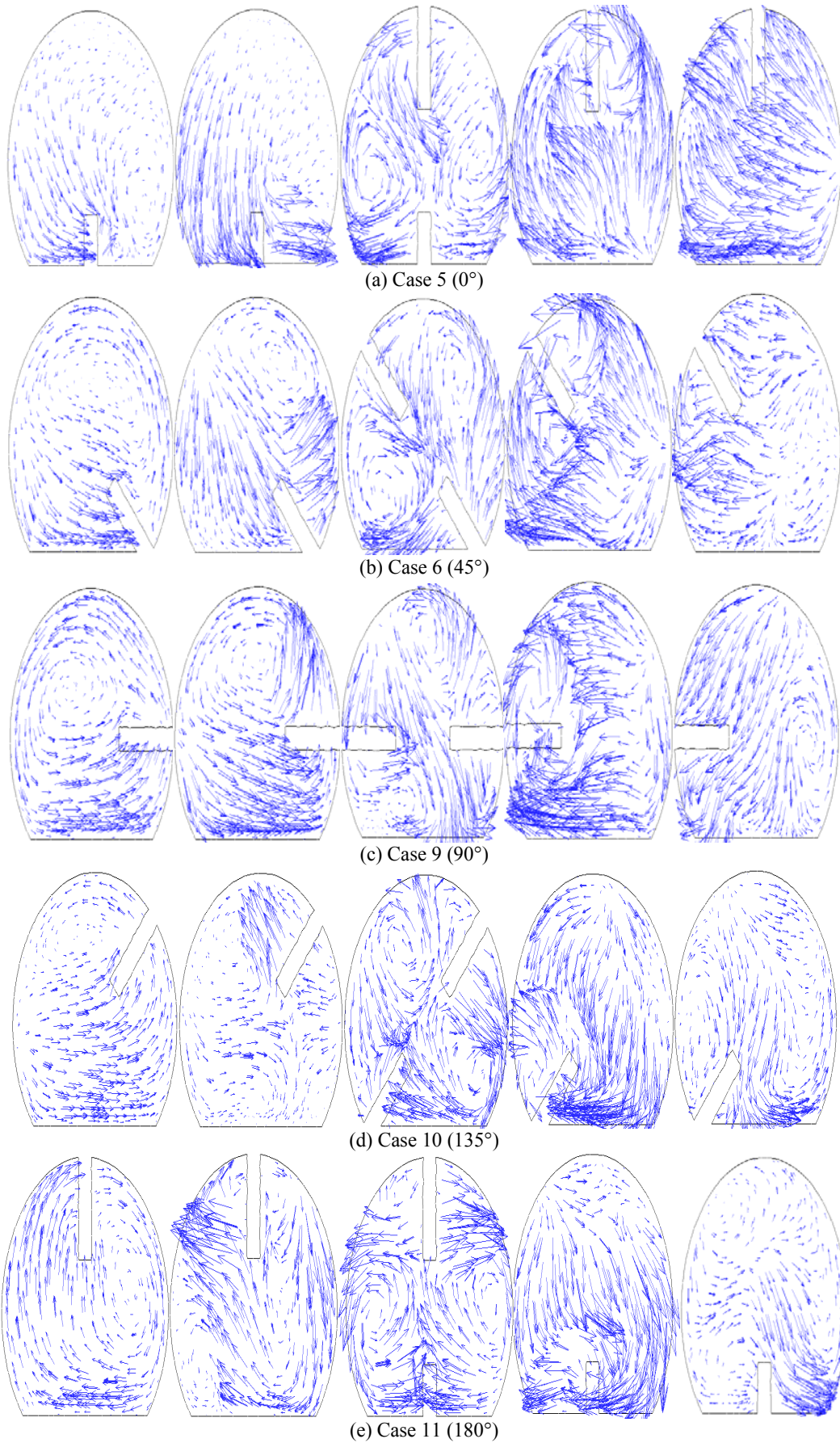


Fig. 16 Velocity profiles at each tertiary air injection location for various rotational angles

CONCLUSIONS

In this study, the computational simulation of petcoke calcination inside a rotary kiln has been conducted using the commercial code FLUENT. The simulations were conducted with different operating conditions and assumptions. The results provide comprehensive information concerning the thermal-flow behavior and combustion inside an industrial rotary kiln. The results show that in the baseline case the peak gas temperature reaches around 1,800 K at $Z/D = 6.6$ in the calcining zone; the lowest gas temperature locates about 1,130 K at $Z/D = 3.6$ between the calcined coke zone and calcining zone; and the exhaust gas temperature at the feed end is approximately 1,150 K. The discharged calcined coke temperature is approximately 1,300 K. The highest coke bed surface temperature is 1,570 K occurring at $Z/D = 6.7$. The typical coke bed temperature difference between surface and bottom varies between 32 and 200 K. For the most part, the coke surface temperature is higher than the bottom temperature, but between $Z/D = 0$ and 6, the coke bottom is hotter than the surface. About 14.22 % of the volatiles (0.776 % of the total mass of gas) are not burned inside the kiln and are carried into the pyroscrubber.

Due to the different tertiary air injection angles, the gas temperatures slightly vary for each rotational angle. The 45° rotational angle case shows a better calcination with 100 K higher bed surface temperature at the discharge end compared to the rest of rotational angles. Without including the coke fines combustion and the coke bed, the lumped gas temperature for the rotational cases shows a peak temperature of 1,400 K at the $Z/D = 2$ due to natural gas combustion; the lowest temperature is around 1,075 K at two locations, $Z/D = 4$ and 8 respectively. The exhaust gas temperature is approximately 1,100K.

ACKNOWLEDGEMENT

This study was jointly supported by Rain CII Carbon, LLC and the Louisiana Board of Regents' Industrial Ties Research Subprogram.